

Study The Effective Dose Equivalent, Flux And LET Spectra On The Surface Of Mars.

Kavita Lalwani^{1*}, Amit Yadav², SreeDevi V.V.³

^{1*,3}Department of Physics, Malaviya National Institute of Technology Jaipur, India

²Department of Electronics and Communication Engineering, RBS Engineering Technical Campus Agra, India

***Corresponding Author:** Kavita Lalwani
Email: kavita.phy@mnit.ac.in

Abstract

The surface of Mars lacks adequate shielding against solar and cosmic radiation, posing a significant challenge for future spacecraft missions to the planet. Understanding the complete space radiation environment, including Galactic Cosmic Radiation (GCR) and Solar Particle Events (SPE), is crucial for developing effective radiation shielding materials. Using OLTARIS simulation, we explore the shielding properties of various materials and Martian regolith to mitigate the potential health risks of ionizing radiation. Additionally, we are examining the effective dose equivalent in multiple organs for different shielding materials and conducting a systematic study of fluence vs. LET spectra to inform the development of suitable shielding solutions.

Key Words: Solar Particle Events, GCR, OLTARIS, Polystyrene, LiH, Kevlar

1. Introduction

In the vacuum of outer space, the environment is characterized by highly ionizing radiation with energy levels reaching several teraelectronvolts (TeV). This type of radiation is unable to reach the Earth's surface due to the planet's magnetic field, which deflects charged particles as they approach. Two primary sources of ionizing radiation in outer space are Galactic Cosmic Rays (GCRs) and Solar Particle Events (SPE). The GCRs [1] originate from energetic sources beyond the solar system, such as stars and supernovae. They are predominantly composed of 85% protons, 13% alpha particles, and completely ionized nuclei of elements with higher atomic numbers. Although particles with high atomic numbers and energy (HZE particles) are less abundant, they can have a significant biological impact. As GCRs originate from outside the solar system, they exhibit isotropic distribution in terms of direction. Solar Energetic Particles (SEPs) [2] are released through energetic processes in the solar corona, such as solar flares and Coronal Mass Ejections (CMEs) [3]. They mainly consist of protons (90-95%), followed by helium nuclei (5-8%) and some heavier nuclei (1%), with variations in composition across different events. SPEs, in general, are unpredictable and often occur during periods of maximum solar activity.

The surface of Mars lacks a strong magnetic field and atmosphere, which means there is less shielding from cosmic radiation than Earth. However, certain factors still lower the amount of radiation on the planet's surface than in free space. The bulk of the Mars surface shields against upward-directed radiation, and the thin Martian atmosphere (1% of Earth's atmosphere) provides some protection from low-energy solar energetic particles (SEPs). Additionally, the direction of incoming solar particles plays a role, as particles near the horizon have to travel through longer paths within the atmosphere than those from near the zenith. Protection from radiation increases at low altitudes, meaning that the amount of radiation will be higher on the top of a mountain than in a crater. The Mars Science Laboratory's (MSL) Radiation Assessment Detector (RAD) instrument [4], which was launched as part of the Curiosity Rover, is currently measuring radiation levels on the surface of Mars. Located inside the Gale Crater, about 4 km deeper than the mean Martian surface, the instrument has been collecting data since August 2012 on charged and neutral particles from galactic cosmic rays (GCR) and solar particle events (SPEs), including both downward and albedo particles [5-7].

When there is a solar particle event, the intensity of the interplanetary magnetic field increases, leading to a reduction in Galactic Cosmic Rays (GCRs). Conversely, during periods of minimum solar activity, the interplanetary magnetic field weakens, intensifying GCRs. Therefore, effective shielding is essential for space travel and missions such as Mars habitation to protect against the impact of GCRs. This paper summarizes the simulation setup used to simulate the GCR and SPE environment on the surface of Mars. Then, the results from the simulation on effective dose equivalent for various shielding materials are discussed. The average dose equivalent in the various organs of a female body is carried out. In addition, Fluence as a function of LET spectra are also studied in simulation.

2. Simulation Set-up in OLTARIS

2.1 Space Radiation Environment

a) Galactic Cosmic Rays on Mars (GCR)

In our OLTARIS project [8], we deliberately chose to utilize the sphere geometry option to design the necessary setup meticulously. This decision was driven by the need to accurately capture the Galactic Cosmic Rays (GCR) spectrum on

the surface of Mars during the 2010 solar minimum event. To achieve this, we strategically employed the Badhwar O'Neill model [9], explicitly considering the MarsGram parameter at an elevation of 0.0 km. In this work, the results have been produced for a one-day mission. Our primary focus was calculating the precise, effective dose equivalent for a female adult voxel (FAX) phantom.

b) Solar Particle Events (SPE)

For the simulation, the solar particle event (SPE) environment is set on the Mars surface, with the event in October 1989, with Mars parameters of MarsGram (MGRAM) and an elevation of 0.0 km. In the simulation, the Dose Equivalent is calculated with quality factor = ICRP 60 [10].

3. Results

3.1 Comparison of Shielding Effectiveness of Various Materials in GCR and SPE Environments:

In OLtaris simulations, the following materials are used as shielding materials, which are listed in Table 1.

S.No.	Material	Chemical Formula	Density (g/cm ³)
1	Lithium Borohydride	LiBH ₄	0.68
2	Lithium Hydride	LiH	0.82
3	HDPE	C ₂ H ₄	0.96
4	Kevlar	C ₁₄ H ₁₄ N ₂ O ₄	1.44
5	Mylar	C ₁₀ H ₈ O ₄	1.38
6	Polypropylene	C ₃ H ₆	0.946
7	Polystyrene	C ₈ H ₈	1.06
8	Aluminium	Al	2.7
9	Boron Nitride	BN	2.1
10	PMMA	C ₅ H ₈ O ₂	1.18
11	Liquid Hydrogen	H ₂	0.071

a) Effective Dose Equivalent

The effective equivalent dose is simulated using 10 g/cm² martian regolith and 1 - 5 g/cm² of a chosen material as radiation shields. We analyzed the effective dose equivalent and observed that liquid hydrogen produced the lowest dose rate. Theoretically, this is obvious as, according to the Bethe-Bloch formula, materials with low atomic number elements and high density have greater stopping power. Thus, liquid hydrogen shows ideal behaviour in radiation shielding. However, it doesn't possess other criteria for a perfect shielding material, such as tensile strength. It is also unstable and difficult to handle.

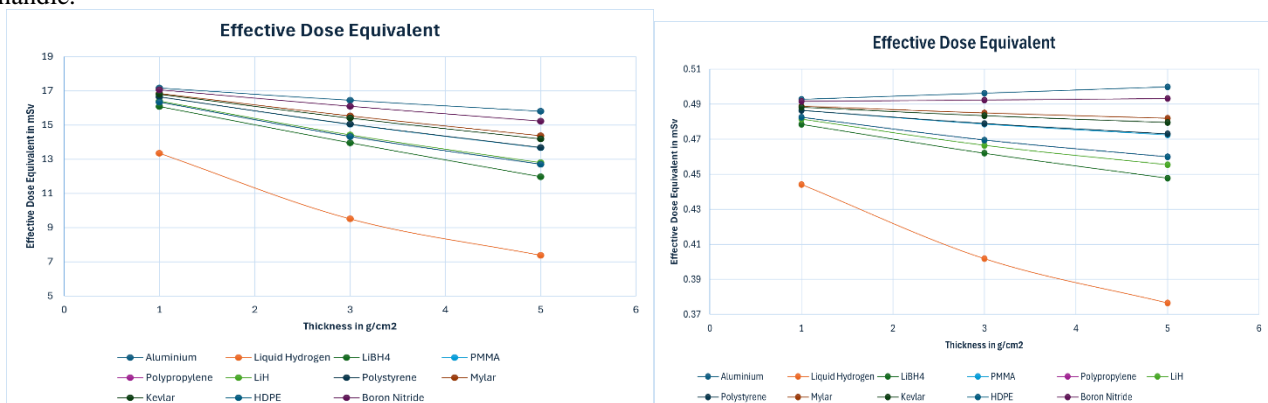


Figure 1: The variation in effective equivalent dose with the thickness (areal density) of various shielding materials in the (left) GCR environment and (right) SPE environment.

Among other materials, LiBH_4 shows the maximum effectiveness. We also find that aluminium and boron nitride do not prove their shielding ability in the GCR environment. Compared with the GCR environment Figure 1(left), dose rates have increased considerably in the SPE environment (Figure 1(right))

3.2 Average Dose Equivalent in Various Organs

The comparison between liquid hydrogen and LiBH_4 results signifies the difference between the maximum achievable dose reduction and the dose reduction achieved in selecting the best shielding material. Compared with figure 2 (left: for the GCR environment), dose rates have increased significantly in the SPE environment (figure 2: right).

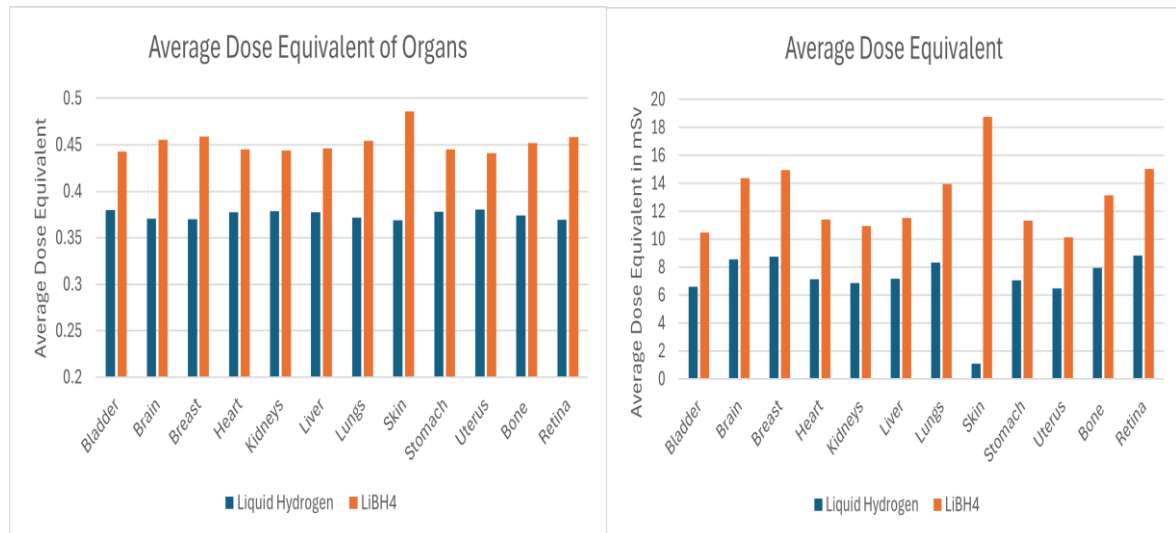


Figure 2: Average dose equivalent in various organs produced by regolith combinations of liquid hydrogen and lithium borohydride in (left) GCR environment and (right) SPE environment.

3.3 Flux vs. Energy

3.3.1 For LiBH_4

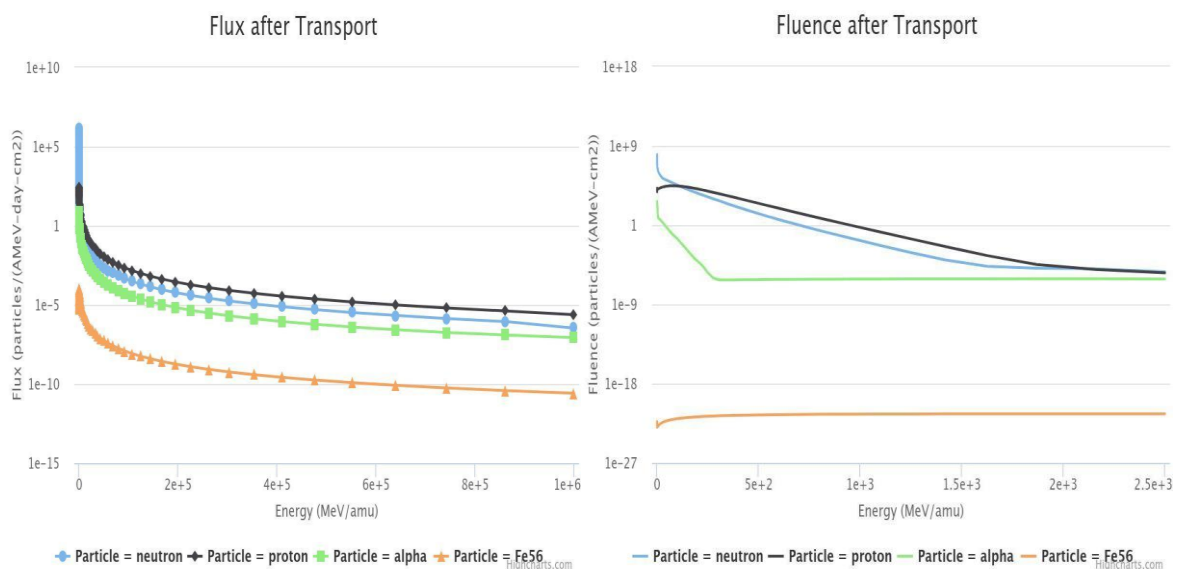


Figure 3: Flux of proton, neutron, alpha particle, and iron at different energies when regolith combination of LiBH_4 is used for shielding in the (left) GCR environment, (right) SPE environment.

It is evident from the plot that the flux of all particles is less at higher energies, and at a particular energy, protons have the highest flux, followed by neutrons, alpha particles, and iron nuclei.

3.3.2 For Liquid Hydrogen

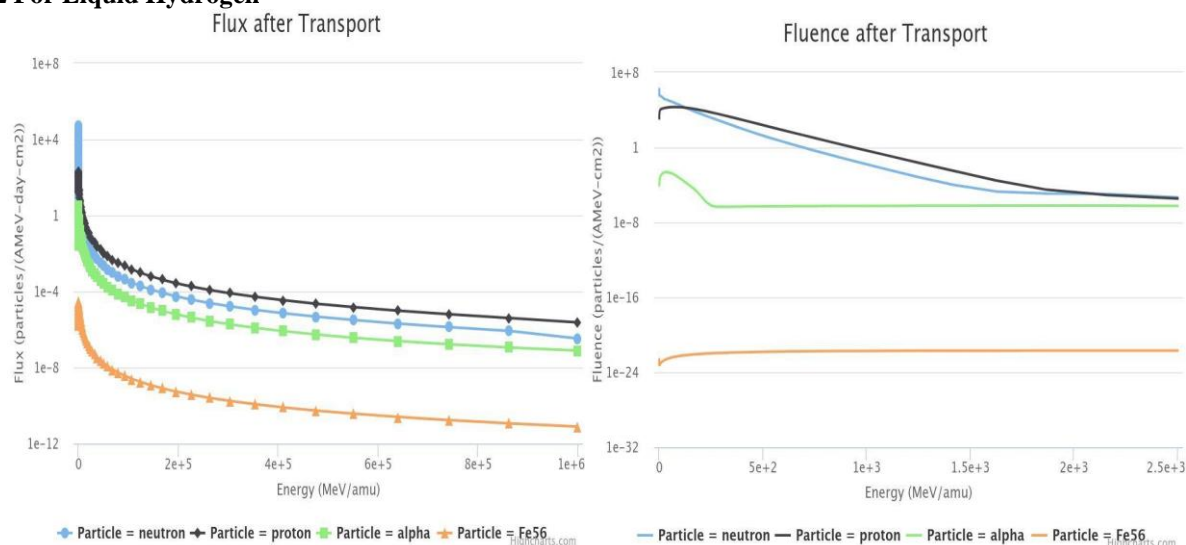


Figure 4: Flux of proton, neutron, iron, and alpha particle at different energies when regolith combination of liquid hydrogen is used for shielding in the (left) GCR environment, (right) SPE environment.

It is evident from the plot that the flux of all particles is less at higher energies, and at a particular energy, protons have the highest flux, followed by neutrons, alpha particles, and iron nuclei, which is expected.

In comparison of figure 3 and figure 4, particle flux is less for liquid hydrogen.

3.4 Differential Flux vs LET for LiBH₄

Variation in the differential flux of all particles with LET (Linear Energy Transfer) when regolith combination of LiBH₄ is used as a radiation shield in the GCR environment (left) and SPE (right). As can be seen from figure 5, there is a rapid decrease in flux of particles with high LET.

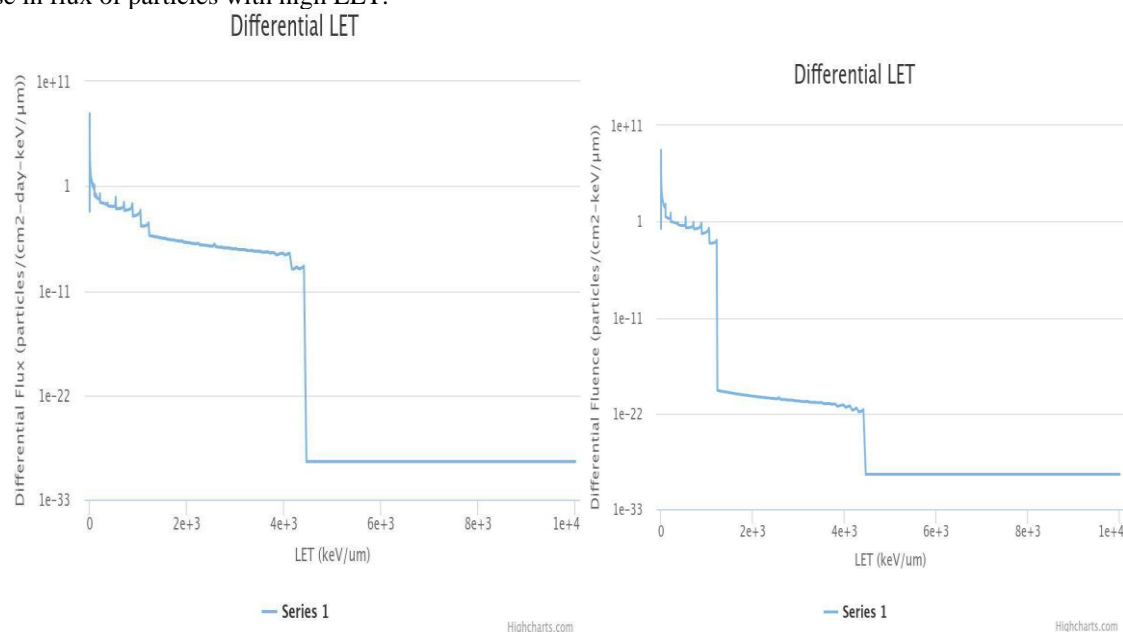


Figure 5: Variation in the differential flux of all particles with LET (Linear Energy Transfer) when regolith combination of LiBH₄ is used as a radiation shield in the GCR environment (left) and SPE (right).

3.5 Differential Flux vs LET for Liquid Hydrogen

Variation in the differential flux of all particles with LET (Linear Energy Transfer) when regolith combination of Liquid hydrogen is used as a radiation shield is shown in figure 6 in the GCR environment (left) and SPE (right).

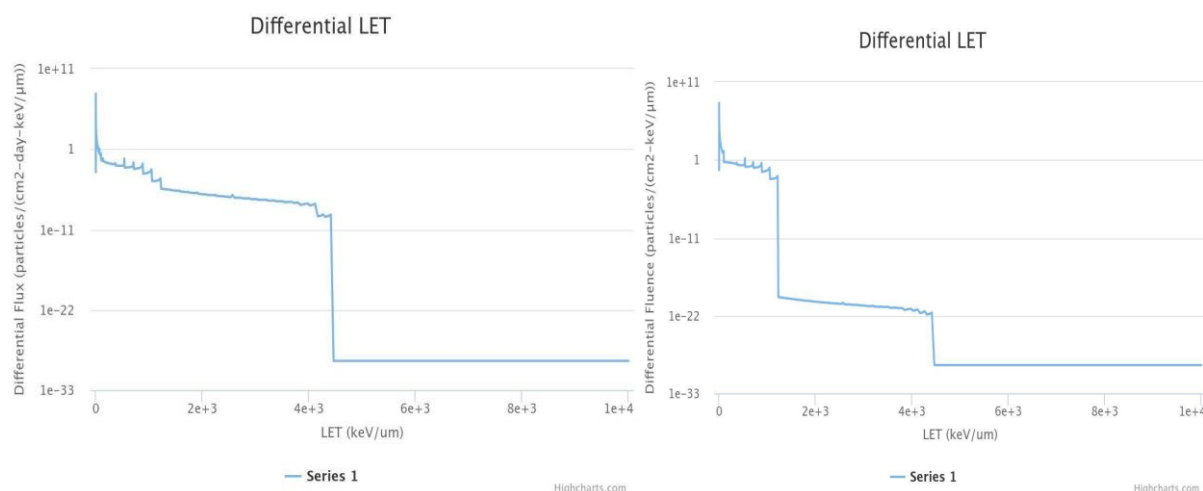


Figure 6: Variation in the differential flux of all particles with LET (Linear Energy Transfer) when regolith combination of liquid hydrogen is used as a radiation shield in the GCR environment (left) and SPE (right).

In comparison with Figure 5, no considerable change is observed in the variation of differential flux with LET as liquid hydrogen is used instead of LiBH_4 .

4. Summary and Conclusion

The research has demonstrated that Liquid hydrogen is a highly effective shielding material for the Mars surface, showing lower absorbed doses than LiBH_4 . Additionally, the simulation of effective dose equivalents for different components of the human female phantom (FAX) using OLTARIS has provided valuable insights. Furthermore, studying LET spectra for all shielding materials in the FAX has contributed to a better understanding of their protective properties. Moreover, the analysis of radiation flux in relation to the energy of incoming radiation/particles has revealed expected trends, with proton radiation flux being higher than alpha and iron, aligning with the GCR environment.

5. References

1. Simpson, J.: Elemental and isotopic composition of the galactic cosmic rays. *Annual Review of Nuclear and Particle Science* 33(1), 323–382 (1983) <https://doi.org/10.1146/annurev.ns.33.120183.001543>.
2. Kallenrode, M.: Current views on impulsive and gradual solar energetic particle events. *Journal of Physics G: Nuclear and Particle Physics* 29(5), 965 (2003) <https://doi.org/10.1088/0954-3899/29/5/316>.
3. Reames, D.V.: Particle acceleration at the sun and in the heliosphere. *Space Science Reviews* 90(3), 413–491 (1999) <https://doi.org/10.1023/A:1005105831781>.
4. Hassler, D.M., Zeitlin, C., WimmerSchweingruber, R., Böttcher, S., Martin, C., Andrews, J., Böhm, E., Brinza, D., Bullock, M., Burmeister, S., et al.: The radiation assessment detector (RAD) investigation. *Space science reviews* 170(1–4), 503–558 (2012) <https://doi.org/10.1007/s11214-012-9913-1>.
5. Ehresmann, B., Zeitlin, C., Hassler, D.M., Wimmer-Schweingruber, R.F., Böhm, E., Böttcher, S., Brinza, D.E., Burmeister, S., Guo, J., Köhler, J., et al.: Charged particle spectra obtained with the Mars Science Laboratory Radiation Assessment Detector (MSL/RAD) on the surface of Mars. *Journal of Geophysical Research: Planets* 119(3), 468–479 (2014) <https://doi.org/10.1002/2013JE004547>.
6. Köhler, J., Zeitlin, C., Ehresmann, B., Wimmer-Schweingruber, R.F., Hassler, D.M., Reitz, G., Brinza, D., Weigle, G., Appel, J., Böttcher, S., et al.: Measurements of the neutron spectrum on the Martian surface with MSL/RAD. *Journal of Geophysical Research: Planets* 119(3), 594–603 (2014) <https://doi.org/10.1002/2013JE004539>.
7. Hassler, D.M., Zeitlin, C., WimmerSchweingruber, R.F., Ehresmann, B., Rafkin, S., Eigenbrode, J.L., Brinza, D.E., Weigle, G., Böttcher, S., Böhm, E., et al.: Mars' surface radiation environment measured with the Mars Science Laboratory's Curiosity rover. *science* 343(6169), 1244797 (2014) <https://doi.org/10.1126/science.1244797>.
8. OLTARIS Document: <https://oltaris.larc.nasa.gov/>
9. 3T. C. Slaba and K. Whitman, "The Badhwar-O'Neill 2020 GCR model," *Space Weather* 18, e2020SW002456, <https://doi.org/10.1029/2020sw002456> (2020).
10. NCRP, Radiation Protection Guidance for Activities in Low-Earth Orbit (National Council on Radiation Protection and Measurements (NCRP), 2000), Issue 132.